Title: The non-thermal effects of pulsed ultrasound irradiation on the development of disuse muscle atrophy in rat gastrocnemius muscle

Authors: Yoko Matsumoto[*], Jiro Nakano[†], Satoshi Oga[*], Hideki Kataoka[‡§], Yuichiro Honda[§], Jyunya Sakamoto[‖], Minoru Okita[§]

Affiliation: [*] Department of Rehabilitation, Saiseikai Nagasaki Hospital
Address: 2-5-1 Katafuchi, Nagasaki-shi, Nagasaki 850-0003, Japan.
Telephone: +81-95-826-9236
Fax: +81-95-827-5657

[†] Unit of Physical and Occupational Therapy, Nagasaki University Graduate School of Biomedical Sciences
Address: 1-7-1 Sakamoto, Nagasaki-shi, Nagasaki 852-8520, Japan.
Telephone and Fax: +81-95-819-7919

[‡] Department of Rehabilitation, Nagasaki Memorial Hospital
Address: 1-11-54 Fukahori, Nagasaki-shi, Nagasaki 851-0301, Japan.
Telephone: +81-95-871-1515
Fax: +81-95-871-1510

[§] Department of Locomotive Rehabilitation Science, Unit of Rehabilitation Sciences, Nagasaki University Graduate School of Biomedical Sciences
Address: 1-7-1 Sakamoto, Nagasaki-shi, Nagasaki 852-8520, Japan.
Telephone and Fax: +81-95-819-7965

‖Department of Rehabilitation, Nagasaki University Hospital
Address: 1-7-1 Sakamoto, Nagasaki-shi, Nagasaki 852-8501, Japan.
Telephone and Fax: +81-95-819-7258

Short title: The non-thermal effects of pulsed ultrasound irradiation on disuse muscle atrophy

Corresponding author: Jiro Nakano
Unit of Physical and Occupational Therapy, Nagasaki University Graduate School of Biomedical Sciences
Address: 1-7-1 Sakamoto, Nagasaki-shi, Nagasaki 852-8520, Japan.
Telephone and Fax: +81-95-819-7919
E-mail: nakano-j@nagasaki-u.ac.jp

Abstract

This study examined the effects of therapeutic pulsed ultrasound (US) on the development of disuse muscle atrophy in rat gastrocnemius muscle. Male Wistar rats were randomly distributed into control, immobilization (Im), sham US, and US groups. In the Im, sham US, and US groups, the bilateral ankle joints of each rat were immobilized in full plantar flexion with a plaster cast for a 4-week period. The pulsed US (frequency, 1 MHz; intensity, 1.0 W/cm^2; pulsed mode 1:4; 15 min) was irradiated to the gastrocnemius muscle in the US group over a 4-week immobilization period. The pulsed US irradiation delivered only non-thermal effects to the muscle. In conjunction with US irradiation, 5-bromo-2'-deoxyuridine (BrdU) was injected subcutaneously to label the nuclei of proliferating satellite cells 1 h before each pulsed US irradiation. Immobilization resulted in significant decreases in the mean diameters of type I, IIA, and IIB muscle fibers of the gastrocnemius muscle in the Im, sham US, and US groups compared with the control group. However, the degrees of muscle fiber atrophy for all types were significantly lower in the US group compared with the Im and sham US groups. Although the number of capillaries and the

concentrations of insulin-like growth factor and basic fibroblast growth factor did not change in the muscle, the number of BrdU-positive nuclei in the muscle was significantly increased by pulsed US irradiation in the US group. The results of this study suggest that pulsed US irradiation inhibits the development of disuse muscle atrophy partly via activation of satellite cells.

Key words: pulsed ultrasound, disuse muscle atrophy, satellite cell, growth factor, capillary, rat

Introduction

Therapeutic ultrasound (US) is a well-established deep-heating modality that converts mechanical energy into a form of sound waves. Therapeutic US, which has been widely used in physical therapy, reduces edema, relieves pain, increases the range of motion, and accelerates tissue repair (van der Windt et al. 1999). It is one of several physical therapy modalities suggested for the management of pain and loss of function due to locomotive syndrome, and it can be used as part of an overall rehabilitation program (Rand et al. 2007). US may be administered in either a continuous or a pulsed mode (Rutjes et al. 2010). Pulsed US produces non-thermal effects and is used to aid in the reduction of inflammation (Johns 2002; Rutjes et al. 2010). The non-thermal effects of pulsed therapeutic US are thought to occur by mechanical stimulation of sound wave to tissues and cells.

On the other hand, mechanical stimulation leads to secretion of insulin-like growth factor (IGF)-1 and other growth factors in skeletal muscle, which play a role in muscle fiber hypertrophy. The secretion of IGF-1 in the muscle fibers

increases within 1h–4 days after muscle fiber was loaded (McKoy et al. 1999; Perrone et al. 1995; Yang et al. 1997). IGF-1 activates protein translation in the ribosome, which increases the muscle fiber volume (Goldspink 1999). In addition, mechanical stimulation loading is known to increase vascular endothelial growth factor (VEGF) and basic fibroblast growth factor (bFGF), which results in the development of more skeletal muscle capillaries (Folkman et al. 1988). An adequate supply of nutrition and oxygen by the increased number of capillaries contributes to muscle fiber hypertrophy and prevents muscle fiber atrophy (Deveci et al. 2002; Nakano et al. 2009; Plyley et al. 1998). Several previous reports regarding the effects of US on cells showed that the irradiation of pulsed US increased VEGF and FGF in fibroblasts and angiogenic cells in culture (Reher et al. 1999; Toyama et al. 2012). Furthermore, low-intensity pulsed US promoted the differentiation of osteoblasts and the proliferation of Schwann cells in culture (Tsuang et al. 2011; Ying et al. 2012), and pulsed US induced an increase in IGF-1 gene expression in undamaged skeletal muscle in humans (Delgado-Diaz et al. 2011). The action of US and the mechanism of hypertrophy induced by mechanical stimulation in concert led us

to hypothesize that pulsed therapeutic US affects muscle fiber size via growth factor secretion or cell proliferation.

Satellite cells, which are undifferentiated myogenic stem cells located between the muscle fiber plasma membrane and the basement membrane, are thought to serve as the source of new muscle fiber nuclei. The importance of satellite cells has been documented during normal muscle growth, regeneration, hypertrophy, and recovery after atrophy (Ambrosio et al. 2009; Gallegly et al. 2004). The application of passive stretch to muscle fibers, i.e., mechanical stimulation, induces an increase in muscle fiber nuclei with enlargement of the muscle fiber size, which is explained by the incorporation of satellite cell nuclei with the adjacent muscle fiber via cell fusion (Carson and Alway 1996; Shenkman et al. 2010). It is not known totally whether the mechanical stimulation by US could affect satellite cells in like a passive stretch.

The effects of therapeutic pulsed US on muscle fiber hypertrophy and atrophy have not been investigated in skeletal muscle and, especially, the influences of pulsed US on satellite cells has not been clarified. If pulsed therapeutic US can induce growth factor release, angiogenesis, and satellite cell

differentiation and/or proliferation in muscle in vivo, then disuse muscle atrophy would be prevented. Therefore, this study examined the effects of pulsed therapeutic US, especially the non-thermal effects, on the development of disuse muscle atrophy in the immobilized hind limbs of rats.

Materials and methods

Animals

All experiments and procedures were approved by the Ethics Review Committee for Animal Experimentation at Nagasaki University. We obtained 62, eight-wk-old, male Wistar rats (220 ± 10 g) from Kudo Laboratories (Tokyo, Japan). The animals were housed in cages inside a room with a 12-h dark/light cycle. The temperature and relative humidity of the room were maintained at 25°C and 50%, respectively. Food and water were available ad libitum.

The previously described animal model of disuse muscle atrophy by cast immobilization (Okita et al. 2004) was used in this study. We randomly distributed 46 rats into 4 groups: control (n = 13), only cast immobilization for 4

weeks (Im, n = 13), pulsed US irradiation during cast immobilization (US, n = 13), and sham US during cast immobilization (sham US, n= 13) groups. Rats in the Im, US, and sham US groups were anesthetized with pentobarbital sodium (40 mg/kg) and their bilateral ankle joints were subsequently fixed in full plantar flexion with plaster casts with the gastrocnemius muscle immobilized in a shortened position. The plaster cast was positioned from above the knee joint to the distal foot. The immobilization period was set for 4 weeks, which was previously shown to be adequate for induction of muscle fiber atrophy (Takekura et al. 1996). Rats in the Im group were immobilized throughout the 4 weeks without treatment. For pulsed US irradiation and sham treatments, bilateral ankle casts in the sham US and US groups were removed under pentobarbital sodium anesthesia (40 mg/kg) during the immobilization period at a frequency of 6 days per week. The bilateral ankle joints were re-immobilized after completion of the daily treatment. The number of rats was not consistent between the groups, because induction of edema by casting and failures of tissue preparation and anesthesia resulted in the exclusion of several rats. Finally, 46 rats were used for analysis of the gastrocnemius muscle

(control, n = 12; Im, n = 9; US, n = 13; and sham US, n = 12).

The remaining 10 rats were used in a pilot study for the measurement of core and muscle temperatures during pulsed US irradiation.

Measurement of core and muscle temperatures during pulsed ultrasound irradiation

The time course changes of core and muscle temperatures were measured during US irradiation in a pilot study. We randomly distributed 10 rats into the US (n = 5) and sham US (n = 5) groups. After the animals were anesthetized with pentobarbital sodium (40 mg/kg), all hair on the right hind limb was subsequently removed and a needle thermo-sensor (PTN-800, Unique Medical Inc., Tokyo, Japan) was carefully inserted in the proximal direction, horizontal to the Achilles' tendon. To target the deep tissue of the gastrocnemius muscle under the US irradiation area, the tip of the needle thermo-sensor was positioned at the center of the triceps muscle of the calf. The diameter of the needle thermo-sensor was 0.6 mm and the needle surface was coated with epoxy for heat insulation. Simultaneously, a cannular thermo-sensor (PTI-200,

Unique Medical Inc., Tokyo, Japan) was inserted 6 cm past the anal sphincter into the colon. Following attachment of the thermo-sensors to a digital thermometer (PTC-301, Unique Medical Inc.), US was irradiated to the gastrocnemius muscle in the right hind limb via the skin for 15 min. The temperature of the experimental room was maintained at 25°C. The core and muscle temperatures were recorded every 1 min for 5 min before irradiation, 15 min during irradiation, and 5 min following irradiation. A sham treatment was carried out while the US device was turned off. The detailed method of US irradiation is described in the following section.

Pulsed ultrasound irradiation

Therapeutic US was applied by using a therapeutic US device (US-750; Itoh Physio-therapy and Rehabilitation Ltd, Tokyo, Japan). We used a probe with a 2-cm diameter, and the effective radiating area (ERA) of this probe was 1.8 cm^2. The US irradiation was performed in pulsed mode at 20% (1:4 duty cycle) to deliver the thermal effects of US to the muscle. An aqueous gel (Aquasonic 100, Parker Laboratories Inc., NJ, USA) served as the US transmission gel. The

gastrocnemius muscle in the US group was irradiated through the shaved skin for 15 min at a frequency of 1 MHz and an intensity of 1.0 W/cm^2.

The US irradiation at the above frequency and intensity should extend to rat gastrocnemius muscle according to previous report (Johnson and O'Brien 2012; Okita et al. 2009; Sakamoto et al. 2012; Tsuang et al. 2011). To deliver US energy to the entire gastrocnemius muscle equally, the US transducer head was moved in a circular fashion over the irradiation area. During US irradiation, the US transmission gel was added as required. In the sham US group, US energy was not delivered to the muscle because the US device was turned off and only the transducer head was moved.

Labeling of muscle nuclei

Mitotically active cells incorporate thymidine analogue 5'-bromo-2'-deoxyuridine (BrdU) into DNA; thus, muscle nuclei, which are post-mitotic, do not incorporate the BrdU label. Labeling with BrdU has been shown to be a reliable technique for distinguishing new muscle nuclei, which could be traced to satellite cells, from all other nuclei (Carson and Alway 1996).

The new muscle nuclei in the gastrocnemius muscle were labeled according to the technique described in our previous study (Nakano et al. 2009). Briefly, all rats in the 4 groups received BrdU (45 mg/kg; Sigma, St Louis, MO, USA) via intraperitoneal injection 1 h before each US irradiation.

Tissue sampling and preparation

At the end of the immobilization period, all rats in the 4 groups were deeply anaesthetized with pentobarbital sodium (40 mg/kg) and the bilateral gastrocnemius muscles were removed. The right muscles were embedded in tragacanth gum, after which the samples were frozen in isopentane cooled by liquid nitrogen and stored in a -80ºC freezer. Serial, 7-μm thick frozen cross-sections of muscle were prepared on a cryostat and were mounted on glass slides for histological and immunohistochemical analysis. Light muscles were immediately cut into 50 mg tissue samples comprised of each of the deep muscle regions. The deep region included both the slow- and fast-twitch fibers. Tissue samples were homogenized in 0.01 M phosphate buffer (PBS; pH 7.4). Homogenates were centrifuged at 4ºC at 5600 g for 10 min and the

supernatants were harvested and stored in a -80ºC freezer. The supernatant solutions were used for ELISA. The amount of protein in each muscle supernatant was determined with a BCA Protein Assay Kit (Pierce, Rockford, IL, USA).

Histochemical analysis of muscle fibers and capillaries

Cross-sections of muscle were evaluated with an optical microscope linked to a video print system and a Windows personal computer. Some muscle cross-sections were stained with hematoxylin and eosin (H&E). Other sections were stained for myosin ATPase activity after acid pre-incubation (pH 4.3), and the adjacent sections were stained for alkaline phosphatase activity. H&E staining was used to identify muscle fiber morphological characteristics and signs of previous muscle injury, such as centralized nuclei. The myosin ATPase reaction served to identify the muscle fiber type (Lind and Kernell 1991). Muscle fiber diameter was determined on at least 100 fibers per major fiber type in the deep regions (type I, IIA, and IIB) with an image analysis computer program (Image J 1.46 software program,

http://rsbweb.nih.gov/ij/download.html). The alkaline phosphatase reaction, which utilized an indoxyl-tetrazolium method, served to visualize the location of the capillaries (Ziada et al. 1984). The capillary supply was evaluated as the capillary-to-muscle fiber ratio (Deveci et al. 2002). In brief, capillaries and muscle fibers were counted in 5 unbiased photographs (×100 magnification; 0.58 mm^2) covering the entire area of the deep regions of the muscle. For each photograph, the capillary-to-muscle fiber ratio was expressed as the number of capillaries per muscle fiber.

Immunohistochemical analysis of and BrdU-positive muscle nuclei

New muscle nuclei that were traced to satellite cells were identified by using double immunostaining with anti-BrdU and anti-dystrophin antibodies. Muscle nuclei are always located inside of the sarcolemma, which is labeled by anti-dystrophin antibody, and new nuclei incorporate BrdU in their DNA. Although fibroblasts and other mitotically active cells in the interstitium also take up the BrdU label, these cells reside outside of the muscle fiber. The BrdU-positive muscle nuclei and muscle fibers were counted on 5 unbiased

photographs (×100 magnification) covering the entire area of the deep regions of muscle. The number of BrdU-positive nuclei per 100 muscle fibers was calculated.

For immunostaining, some cross-sections were air-dried and fixed in ice-cold ether for 10 min. The sections were blocked with 5% bovine albumin in PBS for 60 min. For the first immunostaining, monoclonal anti-dystrophin (1:200 dilution; NCL-DYS1, Novocastra Lab., Britain, UK) was applied to the sections overnight at 4°C. The sections were rinsed in PBS for 15 min, followed by application of the biotinylated goat anti-mouse IgG (1:500 dilution; Vector Lab., CA, USA) for 60 min at room temperature and a second rinse in PBS. The sections were subsequently allowed to react with an avidin–biotin peroxidase complex (VECTASTAINR Elite kit; Vector Lab.) for 30 min at room temperature. Horseradish peroxidase binding sites were visualized as dark brown with 0.05% 3,3′-diaminobenzidine and 0.01% H_2O_2 in 0.5 M Tris-HCl buffer at room temperature. Next, the sections were washed thoroughly in PBS and the second immunostaining was implemented. The sections were treated with 1 N HCl for 60 min at room temperature for DNA denaturation, followed

by washing in PBS. The primary mouse monoclonal anti-BrdU antibody (1:500 dilution; Santa Cruz Biotechnology, CA, USA) was applied to the sections overnight at 4°C. The sections were rinsed in PBS for 15 min, after which biotinylated goat anti-mouse IgG was applied for 30 min at room temperature followed by a second rinse in PBS. Immunoreactivity was visualized as blue with 3,3′,5,5′-tetramethylbenzidine solution (TrueBlue; KPL Inc., Gaithersburg, MD, USA).

Enzyme-linked immunosorbent assay for IGF-1 and bFGF

The levels of IGF-1 and bFGF in the muscles were measured with enzyme-linked immunosorbent assay (ELISA) kits (Quantikine, R&D Systems, Minneapolis, MN, USA) according to the manufacturer's instructions. In brief, the muscle supernatants were incubated on precoated microplates with IGF-1 or bFGF for 2 h at room temperature. After incubation, the microplates were washed and incubated with IGF-1- or bFGF-conjugated horseradish peroxidase for 2 h at room temperature. Subsequently, the microplates were washed and incubated with substrate solution (tetramethylbenzidine/hydrogen peroxide) for

30 min at room temperature in the dark. The reaction was terminated upon the addition of sulfuric acid. Color development was monitored at 450 nm with a microplate reader (Biotec, Bunkyoku, Tokyo, Japan) and the concentrations (in pg/mg) were calculated based on the standard curve.

Statistical analysis

All data are presented as mean ± SD. Differences between groups were assessed by using 1-way analysis of variance (ANOVA) followed by Fisher's PLSD post hoc test. Differences were considered significant at $P < 0.05$.

Results

Core and muscle temperatures

The time course changes in core and muscular temperatures before and during ultrasound irradiation were measured in the pilot study (Fig.1). In the US group, the average core and muscle temperature at 5 min before US irradiation were 36.8 ± 0.5°C and 33.9 ± 1.0°C, respectively. A tendency for the

core temperature to slightly decline was recognized throughout the measurement period, and this was not influenced by US irradiation. Muscle temperature elevation was not observed during and after US irradiation in the US group. Conversely, the muscle temperature was decreased slightly by manipulation of sham US and US irradiation in the sham US and US groups.

Muscle fiber diameter

The development of muscle atrophy was confirmed in the Im, sham US, and US groups, whereas muscle fiber necrosis and regenerating fibers were not observed in the muscles of all groups in the sections stained with H&E (data not shown). Representative photographs of cross-sections stained for myosin ATPase activity (pH 4.3) in the gastrocnemius muscle are shown in Fig. 2A. In the sections stained with myosin ATPase, type I, type IIA, and type IIB fibers were detected in the deep region of the gastrocnemius muscles (Fig. 3B). Quantitative analysis revealed that the muscle fiber diameter of all types in the Im, sham US, and US groups decreased significantly compared with the control group. The diameters of all types of muscle fibers in sham US group showed no

significant differences compared with the Im group. In contrast, the diameters of all types of muscle fibers in the US group were significantly larger than the Im and sham US groups. The decreases in muscle fiber diameter and muscle atrophy were significantly inhibited by pulsed US irradiation in the US group, although the effect was modest.

Capillary and BrdU-positive muscle nuclei

Representative photographs of the alkaline phosphatase reaction (counterstained with eosin) are shown in Fig. 3A. The ratio of the number of capillaries to muscle fiber was significantly decreased in the Im, sham US, and US groups compared with the control group. No difference was observed between the Im, sham US, and US groups (Fig. 3C). Thus, the pulsed US irradiation did not influence the generation of new capillaries.

Representative photographs of double immunostaining for BrdU and dystrophin are shown in Fig.3B. A small number of BrdU-positive nuclei was observed in the Im and sham US groups, and the ratio of the number of BrdU-positive muscle nuclei to muscle fiber was significantly decreased in the

Im and sham US groups compared with the control group. The number of BrdU-positive muscle nuclei was significantly greater in the US group compared to the Im and sham US groups, whereas no difference was observed between the US group and the control group (Fig. 3D).

IGF-1 and bFGF levels

The IGF-1 level was significantly decreased in the Im, sham US, and US groups compared with the control group (Fig. 4A), but no difference was detected among the 3 experimental groups. The bFGF level was not different between any of the 4 groups (Fig. 4B).

Discussion

In this study, the effect of therapeutic US on the development of disuse muscle atrophy was investigated in immobilized rats. Therapeutic US can produce both thermal and non-thermal effects (Rutjes et al. 2010), and the thermal effects are similar to those of general thermal therapy, including pain

relief and acceleration of tissue repair (Xu et al. 1998). However, it is extremely difficult to consider the thermal and the non-thermal effects of continuous US separately. The continuous US produces heat in tissues, whereas the pulsed US does not; therefore, the pulsed US was used in order to evaluate only the non-thermal effect produced by US in this study. In the pilot study, elevations in core temperature and muscle temperature were not observed during pulsed US irradiation. However, the muscle temperature was decreased slightly during and after US irradiation procedure. There is no report that ultrasound irradiation decrease tissue temperature. The decrease in the muscle temperature was not influenced by US irradiation, because the temperature decrease was also observed in the sham US group. The possibility of anesthetic influence is low, because core temperature was not changed in both the sham US and US groups. It was presumably due to a cooling by using ultrasound transmission gel. Although tissues temperature is not heated, the pulsed US (pulsed mode at 20%; 1:4 duty cycle) that was used in this study has slight thermal effects (Locke and Nussbaum 2001). Therefore, we assumed that the decrease in the US group was slighter than that of the sham US group, because

pulsed US irradiation inhibited the decrease of muscle temperature. Several reports showed that low temperature environments could inhibit the development of muscle atrophy (Nagano et al. 2003). In the previous study, the effective low temperature was a room temperature of 8 to 12°C, and this temperature was maintained continuously for 24 hours (Nagano et al. 2003). However, in our pilot study, the decrease of muscle temperature was modest (2 to 3°C), as well as temporary; thus, we believe it is unlikely that this change had an influence on the development of muscle atrophy. We concluded that the changes observed in muscle were due to the influences of the non-thermal effects of the pulsed US.

It is well known that cast immobilization of the hindlimb induces disuse muscle atrophy due to hypodynamia (Takekura et al. 1996). In comparison with the control group, the diameters of type I, type IIA, and type IIB muscle fibers were decreased by 28.2, 28.6, and 30.3%, respectively, in the gastrocnemius muscle of the Im group. Thus, cast immobilization clearly induced disuse muscle atrophy. Although disuse muscle atrophy occurred in both the sham US and US groups, the main finding of this study was that the diameters of all

types of muscle fibers were significantly larger in the US group than in the Im and sham US groups. This finding suggests that the non-thermal effects of the pulsed US inhibited the development of disuse muscle atrophy in the US group partly.

Previous reports showed that the capillary diameter and the number of capillaries were decreased in atrophied muscle because of an inactive and reduced metabolism (Desplanches et al. 1990; Kano et al. 2000; Oki et al. 1999). A decrease in the number of capillaries was also observed in this study because the ratio of the number of capillaries to muscle fiber was decreased significantly in the Im group compared with the control group. The number of capillaries in the US group was not changed compared with the control and sham US groups. Previous studies showed that VEGF, which promotes angiogenesis, was increased by US irradiation in cell culture (Reher et al. 1999; Toyama et al. 2012); further, US irradiation increased VEGF expression in angiogenic cells in vitro (Reher et al. 1999). However, the pulsed US also did not inhibit or prevent the decrease in capillary number with disuse muscle atrophy in the present study. On the other hand, the expression of growth factors such as IGF -1 and

bFGF, which participate in protein synthesis in muscle (Szewczyk and Jacobson 2005), are promoted by mechanical stimulation (Folkman et al. 1988; Perrone et al. 1995). Although we expected that the expression of IGF -1 and the bFGF would be increased by the mechanical stimulation of pulsed US, the concentrations of these growth factors were not changed in the US group. Because bFGF also has effects on angiogenesis (Deindl et al. 2003), our finding that pulsed US irradiation did not affect the bFGF concentration is consistent with the finding that the number of capillaries was not changed by pulsed US irradiation. Therefore, this suggests that the inhibition of disuse muscle atrophy by the non-thermal effects of pulsed US in the US group was not dependent on changes in growth factors and the number of capillaries.

BrdU labeling has been shown to be a reliable technique for distinguishing new muscle nuclei, which are traced to satellite cells, from all other nuclei (Carson and Alway 1996). Thus, the change in the number of BrdU-positive muscle nuclei indicates a change in activated satellite cells. Satellite cells have an important role in the mechanisms of muscle fiber growth and maintenance of size (Wang et al. 2006). The number of BrdU-positive nuclei was decreased in

the Im and sham US groups in this study. Disuse muscle atrophy was confirmed in these 2 groups, suggesting that mechanical stimulation loading to the muscle, which is necessary for the growth and maintenance of muscle fiber size and function, had been decreased. The satellite cell is also activated by mechanical stimulation such as passive stretching (Hawke 2005). Muscle fiber size is thought to depend on the quality of muscle nuclei (Hawke 2005). Therefore, we postulate that the decreases of BrdU-positive nuclei in the Im and sham US groups were caused by the decrease in mechanical stimulation and the development of muscle fiber atrophy (Mozdziak et al. 1998). In contrast, the number of BrdU-positive muscle nuclei in the US group was similar to the control group and was significantly higher than in the Im and sham US groups. When pulsed US was irradiated to the gastrocnemius muscle, the transducer head may have provided mild pressure to the muscle. Although pressure is a form of mechanical stimulation, the number of BrdU-positive nuclei did not change in the sham US group compared with the Im group. Rats in the sham US group and the US group both underwent the procedure with the US device in the switch-off mode. Thus, the increase in number of BrdU-positive muscle

nuclei in the US group was possibly increased due to satellite cell activation from mechanical stimulation, i.e., a non-thermal effect of the pulsed US. Additionally, activated satellite cells differentiate to myoblasts, which proliferate and fuse with the adjacent muscle fiber, contributing to muscle fiber growth (Carson and Alway 1996; Shenkman et al. 2010). Therefore, the activation of satellite cells by the non-thermal effects of pulsed US presumably had an influence on inhibiting the development of disuse muscle atrophy in the US group. It was unclear in this study whether pulsed US activated the differentiation of satellite cells to myoblasts or the proliferation of myoblasts after differentiation. Given that the concentrations of IGF-1 and bFGF in muscle were not changed, we hypothesize that the differentiation of satellite cells was induced by pulsed US directly.

In conclusion, pulsed US irradiation inhibited the development of disuse muscle atrophy by joint immobilization for 4 weeks. Mechanical stimulation by the non-thermal effect of pulsed US might have activated satellite cells, which effectively maintained muscle fiber size. However, this effect was very small and IGF-1 and bFGF levels and the capillaries were not affected. We guess that

the irradiation time of pulsed US was too short to prevent disuse muscle atrophy induced by joint immobilization in the present study. The extension of the irradiation time may increase the effect.

Acknowledgment

The authors thank ITO Co. Ltd. (1-23-15 Shiroyama, Bunkyo-ku, Tokyo 113-0001, Japan) for leasing a therapeutic ultrasound device (US-750) for this study, and Saki Ayabe (Nagasaki Kita Hospital) and Nao Yoshida (Nagasaki Memorial Hospital) for expert technical assistance.

References

Ambrosio F, Kadi F, Lexell J, Fitzgerald GK, Boninger ML, Huard J. The effect of muscle loading on skeletal muscle regenerative potential: an update of current research findings relating to aging and neuromuscular pathology. Am J Phys Med Rehabil 2009;88:145–155.

Carson JA, Alway SE. Stretch overload-induced satellite cell activation in slow

tonic muscle from adult and aged Japanese quail. Am J Physiol 1996;270:C578–C584.

Deindl E, Hoefer IE, Fernandez B, Barancik M, Heil M, Strniskova M, Schaper W. Involvement of the fibroblast growth factor system in adaptive and chemokine-induced arteriogenesis. Circ Res 2003;92:561–568.

Delgado-Diaz DC, Gordon BS, Dompier T, Burgess S, Dumke C, Mazoue C, Caldwell T, Kostek MC. Therapeutic ultrasound affects IGF-1 splice variant expression in human skeletal muscle. Am J Sports Med 2011;39:2233–2241.

Desplanches D, Kayar SR, Sempore B, Flandrois R, Hoppeler H. Rat soleus muscle ultrastructure after hindlimb suspension. J Appl Physiol 1990;69:504–508.

Deveci D, Marshall JM, Egginton S. Chronic hypoxia induces prolonged angiogenesis in skeletal muscles of rat. Exp Physiol 2002;87:287–291.

Folkman J, Klagsbrun M, Sasse J, Wadzinski M, Ingber D, Vlodavsky I. A heparin-binding angiogenic protein--basic fibroblast growth factor--is stored within basement membrane. Am J Pathol 1988;130:393–400.

Gallegly JC, Turesky NA, Strotman BA, Gurley CM, Peterson CA,

Dupont-Versteegden EE. Satellite cell regulation of muscle mass is altered at old age. J Appl Physiol 2004;97:1082–1090.

Goldspink G. Changes in muscle mass and phenotype and the expression of autocrine and systemic growth factors by muscle in response to stretch and overload. J Anat 1999;194 (Pt 3):323–334.

Hawke TJ. Muscle stem cells and exercise training. Exerc Sport Sci Rev 2005;33:63–68.

Johns LD. Nonthermal effects of therapeutic ultrasound: the frequency resonance hypothesis. J Athl Train 2002;37:293–299.

Johnson CA, O'Brien WD, Jr. The angiogenic response is dependent on ultrasound contrast agent concentration. Vasc Cell 2012;4:10.

Kano Y, Shimegi S, Takahashi H, Masuda K, Katsuta S. Changes in capillary luminal diameter in rat soleus muscle after hind-limb suspension. Acta Physiol Scand 2000;169:271–276.

Lind A, Kernell D. Myofibrillar ATPase histochemistry of rat skeletal muscles: a "two-dimensional" quantitative approach. J Histochem Cytochem 1991;39:589–597.

Locke M, Nussbaum E. Continuous and pulsed ultrasound do not increase heat shock protein 72 content. Ultrasound Med Biol 2001;27:1413–1419.

McKoy G, Ashley W, Mander J, Yang SY, Williams N, Russell B, Goldspink G. Expression of insulin growth factor-1 splice variants and structural genes in rabbit skeletal muscle induced by stretch and stimulation. J Physiol 1999;516(Pt 2):583–592.

Mozdziak PE, Truong Q, Macius A, Schultz E. Hindlimb suspension reduces muscle regeneration. Eur J Appl Physiol Occup Physiol 1998;78:136–140.

Nagano K, Kajihara H, Suzaki E, Suzuto M, Kataoka K, Yoshii M, Ozawa K. Disuse atrophy alterations in normal and low temperature environments during hindlimb unloading in Syrian hamsters. Cryo Letters 2003;24:245–252.

Nakano J, Kataoka H, Sakamoto J, Origuchi T, Okita M, Yoshimura T. Low-level laser irradiation promotes the recovery of atrophied gastrocnemius skeletal muscle in rats. Exp Physiol 2009;94:1005–1015.

Oki S, Desaki J, Taguchi Y, Matsuda Y, Shibata T, Okumura H. Capillary changes with fenestrations in the contralateral soleus muscle of the rat

following unilateral limb immobilization. J Orthop Sci 1999;4:28–31.

Okita M, Nakano J, Kataoka H, Sakamoto J, Origuchi T, Yoshimura T. Effects of therapeutic ultrasound on joint mobility and collagen fibril arrangement in the endomysium of immobilized rat soleus muscle. Ultrasound Med Biol 2009;35:237–244.

Okita M, Yoshimura T, Nakano J, Motomura M, Eguchi K. Effects of reduced joint mobility on sarcomere length, collagen fibril arrangement in the endomysium, and hyaluronan in rat soleus muscle. J Muscle Res Cell Motil 2004;25:159–166.

Perrone CE, Fenwick-Smith D, Vandenburgh HH. Collagen and stretch modulate autocrine secretion of insulin-like growth factor-1 and insulin-like growth factor binding proteins from differentiated skeletal muscle cells. J Biol Chem 1995;270:2099–2106.

Plyley MJ, Olmstead BJ, Noble EG. Time course of changes in capillarization in hypertrophied rat plantaris muscle. J Appl Physiol 1998;84:902–907.

Rand SE, Goerlich C, Marchand K, Jablecki N. The physical therapy prescription. Am Fam Physician 2007;76:1661–1666.

Reher P, Doan N, Bradnock B, Meghji S, Harris M. Effect of ultrasound on the production of IL-8, basic FGF and VEGF. Cytokine 1999;11:416–423.

Rutjes AW, Nuesch E, Sterchi R, Juni P. Therapeutic ultrasound for osteoarthritis of the knee or hip. Cochrane Database Syst Rev 2010;20:CD003132.

Sakamoto J, Nakano J, Kataoka H, Origuchim T, Yoshimura T, Okita M. Continuous therapeutic ultrasound inhibits progression of disuse atrophy in rat gastrocnemius muscles. J Phys Ther Sci 2012;24:443–447.

Shenkman BS, Turtikova OV, Nemirovskaya TL, Grigoriev AI. Skeletal muscle activity and the fate of myonuclei. Acta Naturae 2010;2:59–66.

Szewczyk NJ, Jacobson LA. Signal-transduction networks and the regulation of muscle protein degradation. Int J Biochem Cell Biol 2005;37:1997–2011.

Takekura H, Kasuga N, Kitada K, Yoshioka T. Morphological changes in the triads and sarcoplasmic reticulum of rat slow and fast muscle fibres following denervation and immobilization. J Muscle Res Cell Motil 1996;17:391–400.

Toyama Y, Sasaki K, Tachibana K, Ueno T, Kajimoto H, Yokoyama S, Ohtsuka

M, Koiwaya H, Nakayoshi T, Mitsutake Y, Chibana H, Itaya N, Imaizumi T. Ultrasound stimulation restores impaired neovascularization-related capacities of human circulating angiogenic cells. Cardiovasc Res 2012;95:448–459.

Tsuang YH, Liao LW, Chao YH, Sun JS, Cheng CK, Chen MH, Weng PW. Effects of low intensity pulsed ultrasound on rat Schwann cells metabolism. Artif Organs 2011;35:373–383.

van der Windt DA, van der Heijden GJ, van den Berg SG, ter Riet G, de Winter AF, Bouter LM. Ultrasound therapy for musculoskeletal disorders: a systematic review. Pain 1999;81:257–271.

Wang XD, Kawano F, Matsuoka Y, Fukunaga K, Terada M, Sudoh M, Ishihara A, Ohira Y. Mechanical load-dependent regulation of satellite cell and fiber size in rat soleus muscle. Am J Physiol Cell Physiol 2006;290:C981–C989.

Xu LX, Zhu L, Holmes KR. Thermoregulation in the canine prostate during transurethral microwave hyperthermia, Part I: Temperature response. Int J Hyperthermia 1998;14:29–37.

Yang H, Alnaqeeb M, Simpson H, Goldspink G. Changes in muscle fibre type,

muscle mass and IGF-I gene expression in rabbit skeletal muscle subjected to stretch. J Anat 1997;190(Pt 4):613–622.

Ying ZM, Lin T, Yan SG. Low-intensity pulsed ultrasound therapy: a potential strategy to stimulate tendon-bone junction healing. J Zhejiang Univ Sci B 2012;13:955–963.

Ziada AM, Hudlicka O, Tyler KR, Wright AJ. The effect of long-term vasodilatation on capillary growth and performance in rabbit heart and skeletal muscle. Cardiovasc Res 1984;18:724–732.

Figure legends

Fig. 1. Time course changes in core and muscle temperatures before, during, and after irradiation of pulsed US. No increase in core and muscle temperatures was observed during the irradiation. The values represent means ± SD.

Fig. 2. Analysis of muscle fiber diameter in the gastrocnemius muscle. A: Representative photographs of cross-sections stained for myosin ATPase

activity (pH 4.3) are shown. Fibers labeled 1, 2A, and 2B represent type I (dark), type IIA (light), and type IIB (intermediate), respectively. The scale bars represent 50 μm. B: The diameters of all muscle fiber types in the Im, sham US, and US groups decreased significantly compared with the control group and were significantly larger in the US group than the Im and sham US groups. * vs. the control group, † vs. the Im group, ‡ vs. the sham US group ($P < 0.05$ in each). The values represent means ± SD.

Fig. 3. Analysis of capillaries and BrdU-positive nuclei in the gastrocnemius muscle. A: Representative photographs of the alkaline phosphatase reaction (counterstained with eosin) in the US group are shown. Scale bars represent 100 μm. B: Representative photographs of double immunostaining for BrdU and dystrophin in the gastrocnemius muscle in the US group are shown. The anti-dystrophin antibody was used to demonstrate the sarcolemma (arrow) of muscle fibers and the number of BrdU-positive nuclei located inside of the sarcolemma (dark arrowheads) was counted. The right photograph (*) shows a regional enlarged view of the area surrounded by the square in B. The

BrdU-positive nuclei located outside of the sarcolemma (light arrowheads) were excluded from the analysis. Scale bars represent 50 mm. C: No difference was observed in the Im, sham US, and US groups. D: The number of BrdU-positive muscle nuclei in the US group was significantly greater than that of the Im and sham US groups. * vs. the control group, † vs. the Im group, ‡ vs. sham US group ($P < 0.05$ in each). The values represent means ± SD.

Fig. 4. Concentrations of IGF-1 and bFGF in the gastrocnemius muscle. A: IGF-1, B: bFGF. A notable change was not observed in the US group for either of these growth factors. * vs. the control group ($P < 0.05$). The values represent means ± SD.

Fig 1.

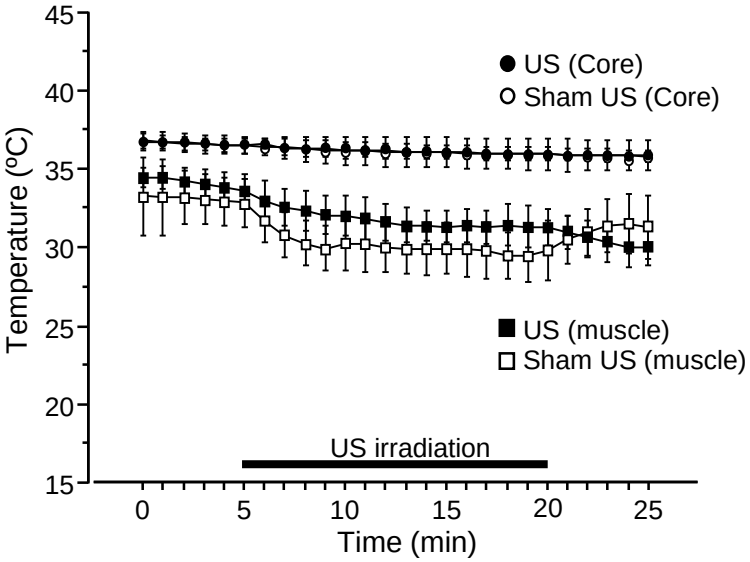
45
40
35
30
25
20
15
Temperature (ºC)
0
5
10
15
20
25
Time (min)
US (Core)
Sham US (Core)
US (muscle)
Sham US (muscle)
US irradiation

Fig 2.

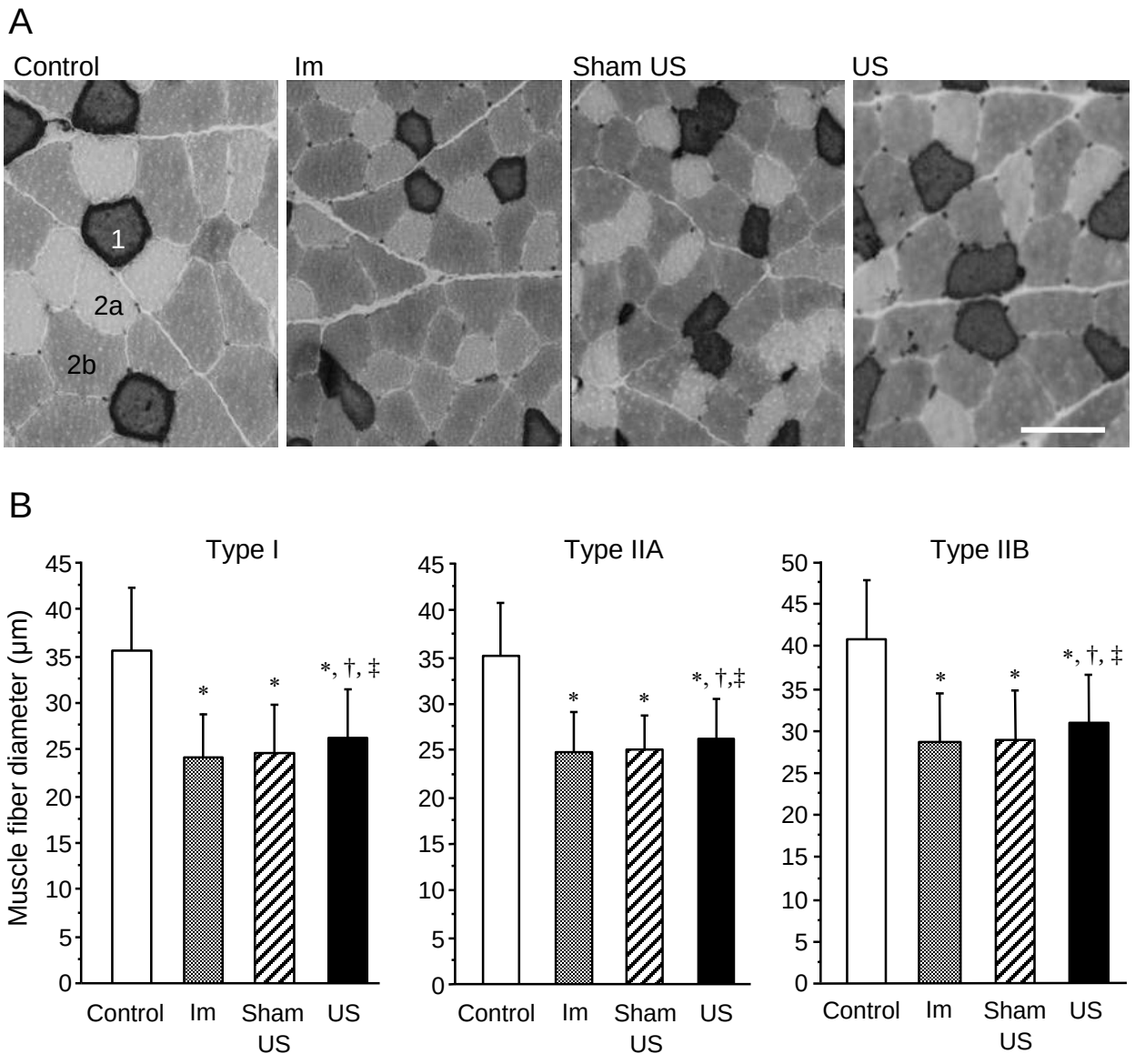
A
Control
Im
Sham US
US
1
2a
2b
B
Type I
Type IIA
Type IIB
Muscle fiber diameter (μm)
Control
Im
Sham US
US
*, †, ‡
*, †,‡

Fig. 3.

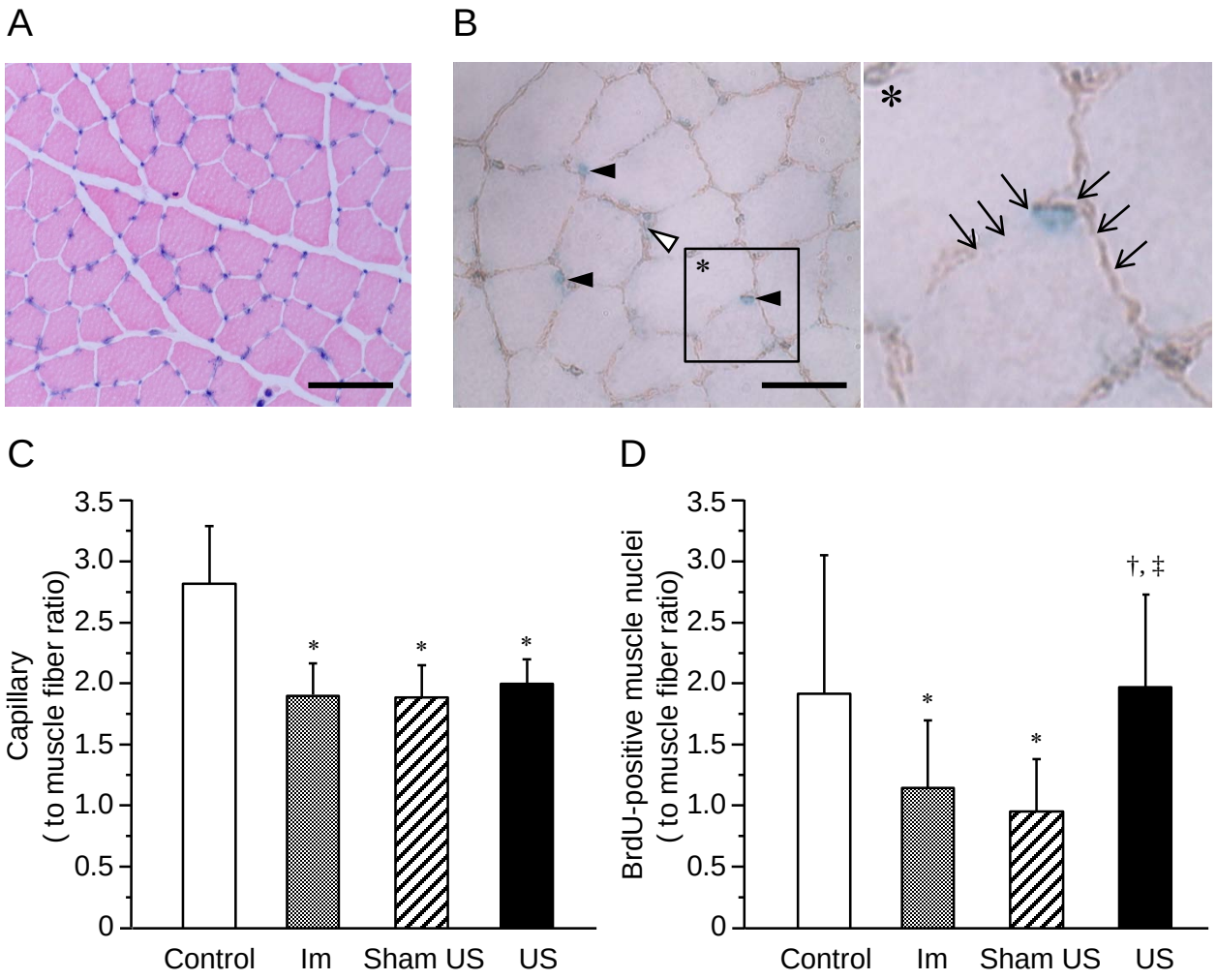
A
B
*
C
Capillary
(to muscle fiber ratio)
3.5
3.0
2.5
2.0
1.5
1.0
0.5
0
Control
Im
Sham US
US
D
BrdU-positive muscle nuclei
(to muscle fiber ratio)
†, ‡

Fig. 4.

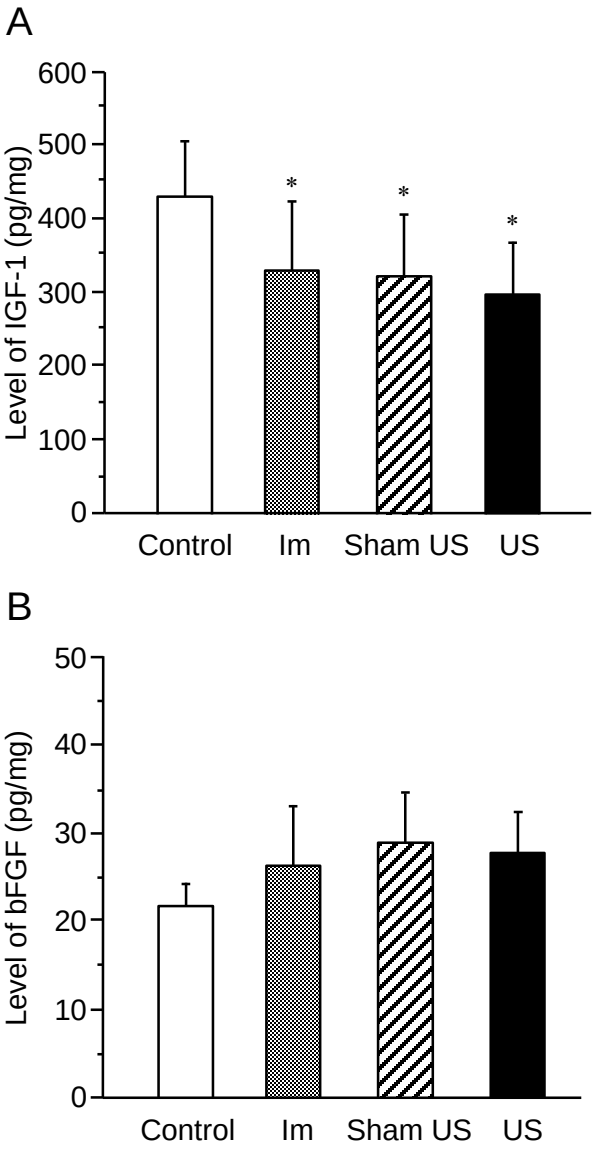
A
Level of IGF-1 (pg/mg)
600
500
400
300
200
100
0
*
*
*
Control
Im
Sham US
US
B
Level of bFGF (pg/mg)
50
40
30
20
10
0
Control
Im
Sham US
US